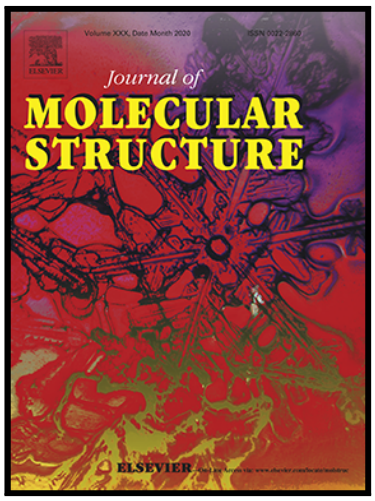

Design and NMR conformational analysis in solution of β5i-selective inhibitors of immunoproteasome

Archimede Rotondo , Maria Zappalà , Santo Previti , Carla Di Chio , Alessandro Allegra , Roberta Ettari

PII: S0022-2860(20)31946-3
DOI: https://doi.org/10.1016/j.molstruc.2020.129633
Reference: MOLSTR 129633

To appear in: *Journal of Molecular Structure*

Received date: 21 October 2020
Revised date: 9 November 2020
Accepted date: 10 November 2020

Please cite this article as: Archimede Rotondo , Maria Zappalà , Santo Previti , Carla Di Chio , Alessandro Allegra , Roberta Ettari , Design and NMR conformational analysis in solution of β5i-selective inhibitors of immunoproteasome, *Journal of Molecular Structure* (2020), doi: https://doi.org/10.1016/j.molstruc.2020.129633

Highlights

- The study is based on the synthesis of β5i-selective and effective inhibitors of proteasome and immonoproteasome as effective potential drugs.
- The activity of some pyridone derivates endowed with peptide mimicking moieties is explored to design drugs.
- Among this group, one allyl and phenylalanine peptide analogue turned out to be more effective.
- The NMR conformational analysis demonstrated that the most active compound is the most rigid in the apolar media.
- This conformational behaviour may account for the enhanced activity of the chemical because of specific biological interactions.

Design and NMR conformational analysis in solution of β5i-selective inhibitors of immunoproteasome

Archimede Rotondo*[a], Maria Zappalà[b], Santo Previti[b], Carla Di Chio[b], Alessandro Allegra[c] and Roberta Ettari*[b]

[a]*Department of Biomedical Sciences, Dentistry and Morphological and functional Immages - BIOMORF, University of Messina, Viale Annunziata, 98168 Messina, Italy. E-mail: arotondo@unime.it*

[b]*Department of Chemical, Biological, Pharmaceutical and Environmental Sciences, University of Messina, Viale Annunziata, 98168 Messina, Italy. E-mail: rettari@unime.it*

[c]*Department of Human Pathology in Adulthood and Childhood, University of Messina, Via C. Valeria, 98125 Messina, Italy.*

*Corresponding author: Tel +39-090-6766890, Fax +39-090-393756

e-mail address: arotondo@unime.it; rettari@unime.it

Abstract

The identification of effective and selective immunoproteasome inhibitors could greatly promote smart treatment of many autoimmune, inflammatory and tumor diseases. This paper explores the activity of some pyridone derivatives which are taking advantage of peptide mimicking moieties and other functional groups whose related effects are taken into consideration. The target compounds were designed and synthesized starting from a lead, next their *in vitro* biological activity was tested; the following structural and conformational analysis sheds light over the different activity of the tested compounds. Compound **3** bearing a phenylalanine at the P2 site and an allyloxycarbonyl group spanning the P3 region, was found to be a selective inhibitor of β5 subunit of immunoproteasome. It has been demonstrated by Nuclear Magnetic Resonance (NMR) that, in solution, this substrate displays a more rigid conformation respect to the others, especially in apolar media, this feature is likely crucial for the enhancement of the activity towards immunoproteasome. The specific conformational analysis enables insights of the biological activity of new chemicals driving possible advancements based on the suitable structural features to identify novel selective β5 immunoproteasome inhibitor.

KEYWORDS: Immunoproteasome; Amide derivatives; noncovalent inhibitors; NMR; Conformational analysis.

1. Introduction

The 20S proteasome is the most relevant non-lysosomal proteolytic system in eukaryotic cells, being involved in the degradation of most cellular proteins [1-2]. Tumor cells are strictly dependent on proteasomal function, thus proteasome inhibition represents a novel therapeutic strategy to kill cancer cells [3-7]. The 26S proteasome possesses a central 20S catalytic core characterized by a barrel-like structure, with the two outer and the two inner rings composed of seven different α- and β-subunits, respectively. β1c, β2c and β5c are the constitutive core particles (cCPs), responsible for the caspase-like (C-L), trypsin-like (T-L) and chymotrypsin-like (ChT-L) activities, respectively [8]. Another specialized form of proteasome, mainly expressed in lymphocytes and monocytes is represented by the immunoproteasome. Under the stimuli of IFN-γ and TNF-α, the cCPs are replaced by the immuno-core particles (iCPs) β1i, β2i, and β5i subunits, respectively. While β5i and β2i subunits maintain the same activities of the constitutive counterparts, β1i subunit performs a chymotrypsin-like activity, while its caspase-like activity is reduced to background levels [9]. An up-regulation of immunoproteasome has been detected in a large number of autoimmune diseases, like rheumatoid arthritis or systemic lupus erythematosus and in a panel of inflammatory diseases, such as Crohn's and inflammatory bowel or ulcerative diseases, as well [10]. At the same time, iCPs are overexpressed in hematopoietic cells, including multiple myeloma (MM) cells, thus selectively targeting iCPs could be an innovative strategy in the drug discovery process of new agents for the treatment of hematologic malignancy [11-13]. In the last years, many efforts have been made to develop noncovalent proteasome or immunoproteasome inhibitors, which may lack of several off targets effects with respect to the irreversible inhibitors of human proteases [14-17]. In this context, our research group has been actively involved in the development of novel 20S proteasome [18-23] and immunoproteasome [24-25] inhibitors endowed with K_i values in the submicromolar range. Starting from the lead compound **1** [25], which inhibited β5c subunit more effectively than the β5i counterpart (K_i=8.8 μM and 45.5 μM, respectively), we decided to extend the P3 site with the introduction of a moiety potentially able to act as H-bond donor and/or H-bond acceptor, thus we functionalized the amino group at position 3 of the

pyridin-2(1*H*)-one nucleus into a carbamate function, i.e. compounds **2-3 (**Fig. **1**). At the P2 site, for which no specificity is assessed, we first maintained the P2 phenylalanine (Phe) residue, later studying the impact upon the activity driven by the replacement of this residue with leucine (Leu). Finally, the isopentyl group was introduced as capping substituent of the amide moiety in order to match the structural features of the S1 pockets of β1i and β5i subunits, which are large and hydrophobic [12]. Compound **4** was subsequently synthesized as an optimization process of the most active of the two inhibitors. We now report and discuss the synthesis, biological investigation and conformational analysis of the three synthesized potential inhibitors of immunoproteasome.

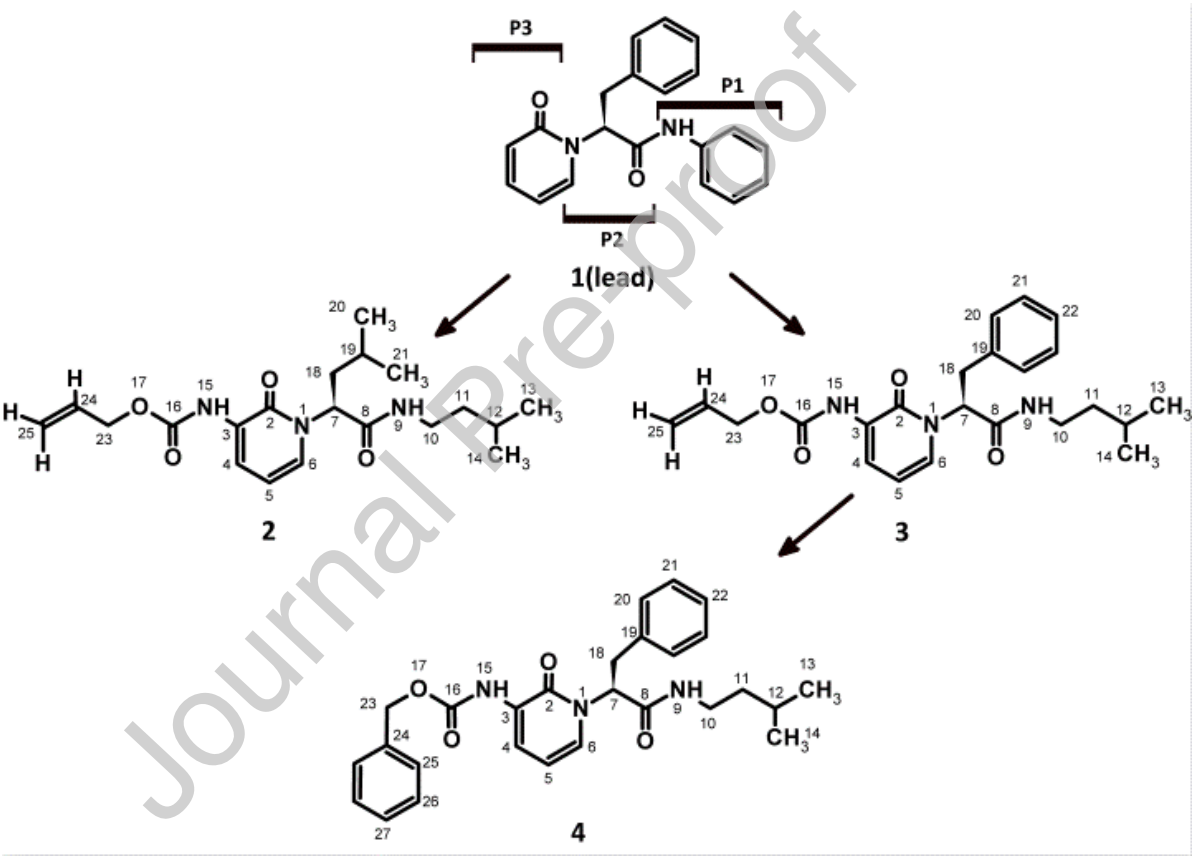

Fig. 1. Molecular representation and labeling scheme of the studied compounds.

2. Results and Discussion

2.1. Synthesis

The synthesis of novel peptidomimetics **2-4** (Scheme 1) was carried out following a synthetic strategy widely validated in our laboratories [18]. The commercially available 3-aminopyridin-2(1H)-one nucleus was first protected at the amino group with allyl or benzyl chloroformate to give intermediates **5-6**; in parallel, Leu and Phe (*R*)-α-hydroxy ester derivatives were treated with mesyl

chloride, allowing us to obtain the corresponding mesylate analogues **7-8**; *N*-alkylation of **5-6** with mesylates **7-8** gave the dipeptide analogues with inversion of the stereochemical configuration, according to the SN2 mechanism. Subsequently, their hydrolysis in alkaline condition via LiOH gave the acids **9-11** [18], which were coupled to the commercially available isopentylamine. Coupling reactions were performed in dry DCM/DMF (1:1) using HOBt/EDCI as coupling reagents and DIPEA as a base. The resulting crudes were purified by preparative HPLC providing the desired products **2-4** in good yields (68-77%).

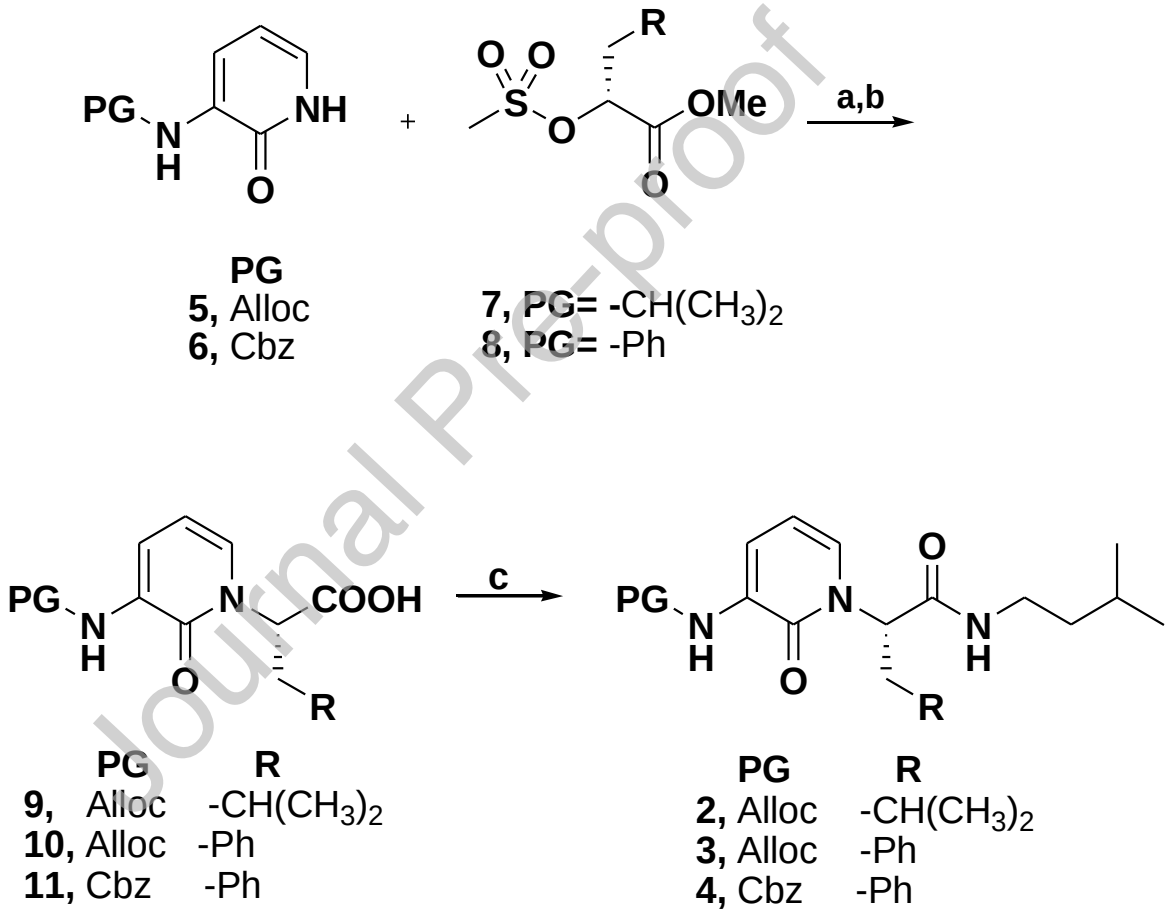

Scheme 1. Reagents and conditions. a) NaH, DMF, 0°C, 1 h, N_2; then **7-8**, rt, 12h; b) LiOH, MeOH/H_2O (1:1), rt, 5 h; c) HOBt, EDCI, dry DCM/DMF (1:1), 0°C, N_2; then isopentylamine, DIPEA, rt, 12h.

2.2. Biological activity

All the three synthesized compounds were tested for their ability to inhibit each one of the catalytic subunits of c20S and i20S, by measuring the rate of hydrolysis of the appropriate fluorogenic substrate (Suc-Leu-Leu-Val-Tyr-AMC for β5i and β5c; Boc-Leu-Arg-Arg-AMC for β2i and β2c; Ac-Pro-Ala-

Leu-AMC for β1i and Z-Leu-Leu-Glu-AMC for β1c). MG-132 (Z-Leu-Leu-Leu-al), a reversible inhibitor of both proteasome and immunoproteasome, was used as positive control. First, compounds underwent a preliminary screening on each proteolytic subunit at 100 μM. Compounds able to inhibit the enzymatic activity by more than 60% were characterized in detail. Continuous assays were thus performed (progress curve method, at seven different concentrations, ranging from those that minimally inhibited to those that fully inhibited the immunoproteasome or the proteasome subunit) to determine the K_i values reported in Table **1**.

Table 1. Activity on proteasome and immunoproteasome core-particles of compounds **1-4**

% of inhibition at 100 μM or K_i (μM)[a]						
Comp.	β1c	β2c	β5c	β1i	β2i	β5i
1[23]	15%	6%	8.8±1.1	23%	n.i.	45.5± 2.6
2	26%	n.i.	36%	7%	8%	16%
3	24%	n.i.	33%	2%	3%	33.6±0.2
4	13%	n.i.	23%	n.i.	n.i.	5%

[a] For K_i values, data represent the mean ± SD of two independent determinations, each performed in duplicate. n.i.=no inhibition.

Between the two initially synthesized Alloc-derivatives **2-3**, only compound **3,** bearing a Phe residue at the P2 site, turned out to be active against immunoproteasome, with a total selectivity against β5i subunit showed by a K_i value of 33.6 μM, thus suggesting a key role of the P2 Phe in the interaction with the target enzyme. With respect to the lead compound **1**, compound **3** showed both an increase of the activity against β5i subunit and of the selectivity over the constitutive counterpart β5c. With the aim to optimize the identified selective immunoproteasome inhibitor **3**, also compound **4** bearing a Cbz *N*-protecting group was synthesized, in such a way to evaluate if the additional aromatic nucleus could establish additional interactions with the S3 pocket of immune-core particles, however this structural modification turned out to be unfruitful.

2.3. Conformational analysis

In order to better understand the features leading to the sole activity and selectivity of compound **3** against immunoproteasome the three similar compounds **2-4** were totally characterized by homo and heteronuclear ^{1}H, ^{13}C and ^{15}N NMR and assignments are reported in **Tables 2-4;** relative spectra with the structural features are illustrated in **Fig. 2** and **3**. Beyond the definite structural elucidation, NMR

data enables the conformational analysis of these species in different media (mimicking *in vivo* drug behaviour in polar and apolar environments); it accounts for specific biological activities possibly improved constructs by de novo design [23, 26, 27].

Table 2. Chemical shift (in ppm) recorded for ^{13}C and ^{15}N hetero nuclei (X) and hydrogen nuclei belonging to the molecule **2** in $CDCl_3$ and in CD_3OH. Delta values indicate chemical shift deviation in ppm respect to expected values calculated on the basis of a wide database of compounds. Remarkable deviations from expected values are indicated in gray, for compound **3** these values in $CDCl_3$ are somewhat bigger according to a pretty locked conformation.

	Compound **2** in $CDCl_3$				Compound **2** in CD_3OH			
XHn	X Shift	X Delta	H shift	H Delta	X Shift	X Delta	H shift	H Delta
2-C	157.41	-0.23	-	-	158.90	1.26	-	-
3-C	129.04	0.48	-	-	129.75	1.20	-	-
4-CH	120.55	-3.78	8.024	0.087	122.52	-1.82	7.991	0.054
5-CH	107.51	-4.04	6.314	-0.016	107.32	-4.23	6.384	0.054
6-CH	126.02	-2.54	7.183	-1.018	128.67	0.10	7.397	-0.804
7-CH	56.15	-0.92	5.526	0.492	57.19	0.12	5.643	0.609
8-C	n.d	n.d	-	-	171.68	2.97	-	-
10-CH_2'	38.13	1.49	3.156	-0.118	38.80	2.16	3.199	-0.075
10-CH_2"	38.13	1.49	3.248	-0.026				
11-CH_2	38.20	-0.36	1.337	-0.029	39.08	0.52	1.369	0.003
12-CH	25.80	-0.72	1.509	-0.048	26.62	0.10	1.565	0.008
13,14-CH_3	22.36	-0.43	0.864	-0.062	22.48	-0.31	0.891	-0.035
16-C	153.31	-0.41	-	-	155.18	1.46	-	-
18-CH_2'	38.83	-0.59	1.995	0.129	40.95	1.53	1.890	0.024
18-CH_2"	38.83	-0.59	1.830	-0.036				
19-CH	24.82	-0.60	1.430	-0.189	25.84	0.42	1.388	-0.231
20-CH_3	22.56	0.22	0.931	0.052	21.73	-0.61	0.928	0.049
21-CH_3					23.11	0.77	0.944	0.065
23-CH_2	66.15	0.12	4.675	0.052	66.69	0.66	4.655	0.032
24-CH	132.59	0.69	5.959	0.085	133.56	1.67	5.990	0.116
25-CH_2c	118.53	0.29	5.266	-0.014	118.13	-0.10	5.232	-0.048
25-CH_2t	118.53	0.29	5.368	0.003	118.13	-0.10	5.361	-0.004
1-N	172.58	18.43	-	-	Nd	nd	-	-
9-NH	117.39	7.43	6.296	-0.477	Nd	nd	8.264	1.491
15-NH	96.14	-1.98	7.806	-0.677	Nd	nd	8.233	-0.250

Dashes indicate missing resonances, nd in instead used for "not detected" signals probably due to the lack of sensitivity

Table 3. Chemical shift (in ppm) recorded for ^{13}C and ^{15}N hetero nuclei (X) and hydrogen nuclei belonging to the molecule **3** in $CDCl_3$ and in CD_3OH. Delta values indicate chemical shift deviation in ppm respect to expected resonances calculated on the basis of a wide database of compounds. Remarkable deltas are indicated in gray, for compound **3** these values in $CDCl_3$ are somewhat bigger according to a pretty locked conformation

	compound **3** in $CDCl_3$				compound **3** in CD_3OH			
XHn	X Shift	X Delta	H Shift	H Delta	X Shift	X Delta	H Shift	H Delta
2-C	157.23	-0.24	-	-	158.21	0.74	-	-
3-C	128.92	-0.39	-	-	130.22	0.91	-	-
4-CH	120.24	-3.59	8.000	0.048	122.58	-1.24	7.930	-0.022
5-CH	107.17	-4.04	6.300	0.146	107.31	-3.90	6.322	0.168
6-CH	125.87	-4.15	7.296	-1.208	129.25	-0.77	7.476	-1.028
7-CH	59.27	-1.85	5.671	0.627	60.65	-0.47	5.746	0.702
8-C	167.98	-0.66	-	-	170.45	1.81	-	-
10-CH_2"	37.90	1.71	3.220	-0.087	38.63	2.45	3.129	-0.178
10-CH_2'			3.117	-0.190			3.179	-0.128
11-CH_2	38.00	-0.40	1.244	-0.049	38.76	0.36	1.295	0.002
12-CH	25.63	-0.88	1.387	-0.170	26.50	-0.02	1.443	-0.114
13/14-CH_3	22.37	-0.42	0.820	-0.106	22.45	-0.33	0.854	-0.072
16-C	153.22	-0.49	-	-	154.75	1.04	-	-
18-CH_2"	36.40	0.15	3.541	0.307	37.81	1.56	3.192	-0.042
18-CH_2'			3.111	-0.123			3.434	0.2
19-C	135.85	-1.40	-	-	137.49	0.24	-	-
20-CH	129.05	-0.73	7.195	-0.027	130.66	0.87	7.195	-0.027
21-CH	128.70	0.41	7.260	-0.050	129.84	1.54	7.223	-0.087
22-CH	127.02	0.83	7.217	0.130	127.84	1.65	7.169	0.082
23-CH_2	65.89	-0.14	4.662	0.039	66.70	0.67	4.636	0.013
24-CH	132.22	0.33	5.951	0.077	133.75	1.86	5.976	0.102
25-CH_2c	118.27	0.03	5.262	-0.018	118.14	-0.10	5.228	-0.052
25-CH_2t			5.360	-0.005			5.347	-0.018
9-NH	119.66	9.50	6.111	-0.884	n.d	n.d	8.167	1.172
15-NH	96.26	-1.91	7.751	-0.846	n.d.	n.d.	8.189	-0.408

Dashes indicate missing resonances, nd is instead used for "not detected" signals probably due to the lack of sensitivity

Table 4. Chemical shift (in ppm) recorded for ^{13}C and ^{15}N hetero nuclei (X) and hydrogen nuclei belonging to the molecule **4** in $CDCl_3$ and in CD_3OH. Delta values indicate chemical shift deviation in ppm respect to expected resonances calculated on the basis of a wide database of compounds. Remarkable deltas are indicated in gray, for compound **4** these values in $CDCl_3$ are somewhat more respect to compound **2** but less pronounced respect to the records concerning compound **3**.

	compound **4** in $CDCl_3$				compound **4** in CD_3OH			
Atom type and label	X Shift	X Delta	H Shift	H Delta	X Shift	X Delta	H Shift	H Delta
2-C	157.20	-0.19	-	-	158.35	0.96	-	-
3-C	128.94	-0.10	-	-	129.75	0.72	-	-
4-CH	120.32	-3.13	8.016	0.149	122.46	-0.99	7.940	0.073
5-CH	107.19	-4.02	6.298	0.144	107.17	-4.04	6.319	0.165
6-CH	126.00	-4.02	7.303	-1.201	129.09	-0.92	7.470	-1.034
7-CH	59.26	-1.87	5.664	0.620	60.75	-0.38	5.735	0.691
8-C	167.95	-0.69	-	-	170.17	1.53		0.000
10-CH_2'	38.01	1.82	3.206	-0.101	38.70	2.51	3.123	-0.184
10-CH_2''	38.01	1.82	3.110	-0.197	38.70	2.51	3.183	-0.124
11-CH_2	38.03	-0.37	1.246	-0.047	38.76	0.36	1.286	-0.007
12-CH	25.64	-0.88	1.384	-0.173	26.37	-0.15	1.440	-0.117
13-CH_3	22.32	-0.47	0.811	-0.115	22.46	-0.33	0.846	-0.080
14-CH_3	22.36	-0.43						
16-C	153.29	0.33	-	-	154.86	1.90	-	-
18-CH_2'	36.45	0.20	3.095	-0.139	37.74	1.49	3.194	-0.040
18-CH_2''	36.45	0.20	3.530	0.296	37.74	1.49	3.425	0.191
19-C	135.85	-1.40	-	-	137.12	-0.13	-	-
20-CH	129.12	-0.66	7.190	-0.032	129.90	0.12	7.193	-0.029
21-CH	128.72	0.43	7.250	-0.060	129.26	0.97	7.211	-0.099
22-CH	127.14	0.95	7.216	0.129	127.72	1.53	7.166	0.079
23-CH_2	67.16	0.37	5.198	0.069	67.74	0.95	5.177	0.048
24-C	135.91	-0.52	-	-	137.43	1.01	-	-
25-CH	128.65	0.12	7.380	0.059	128.84	1.28	7.396	-0.016
26-CH	128.23	0.67	7.389	-0.023	129.26	0.73	7.361	0.040
27-CH	128.41	0.80	7.349	0.155	128.96	1.34	7.325	0.131
1-N	172.63	24.13	-	-	172.60	24.09	-	-
9-NH	119.75	9.59	6.158	-0.837	121.75	11.58	8.154	1.159
15-NH	96.66	-5.82	7.780	-0.958	95.76	-6.72	8.211	-0.527

Dashes indicate missing resonances, nd in instead used for "not detected" signals probably due to the lack of sensitivity

As demonstrated in other similar cases, compounds **2**, **3** and **4** in polar and protic solvents (CD_3OH) display a greater conformational freedom, whereas, in apolar environments ($CDCl_3$) data confirm the permanent presence of intramolecular interactions [26] eliciting limited molecular

arrangements. Any information about conformational features [28, 29] and kinetic freedom [30] is crucial to understand the possible efficacy of drugs, since it provides the descriptors shared as the basement for any leads [31]. In this case, all the NMR data (see below and supporting information) are consistent with the presence of a prevailing conformation in $CDCl_3$ stabilized by intramolecular dipolar interactions; this conformation is very close to the minimized models obtained through optimization calculations. The detected stiffness concerns the N1-C7-C8-N9 and C3-N15-C16 frameworks connected to the pyridone core ring, however, only for compounds **2** and **4**, some space contacts (NOE NMR) reveal the allowed rotation through the N1-C7 dihedral angle. It is not the case of compound **3** which also present more defined elements featuring the prevalent conformation represented in Fig. 3 and reported in details into the supplementary text**.** On the other hand, all the three molecules display some dynamic freedom concerning the peripheral chains attached to the 10-CH_2 and 23-CH_2 knots, this fluxional behavior is enhanced in CD_3OH and involves also the core structure by the weakening of intramolecular interactions replaced by the intermolecular interactions (solvation). On the basis of the mentioned basic knowledge about drugs, the less pronounced conformational freedom of **3** in apolar solvents accounts for its enhanced activity towards the biological substrate, whereas the conformational changes in polar media will guarantee the necessary drug ability to kinetically fit in to the bioactive site.

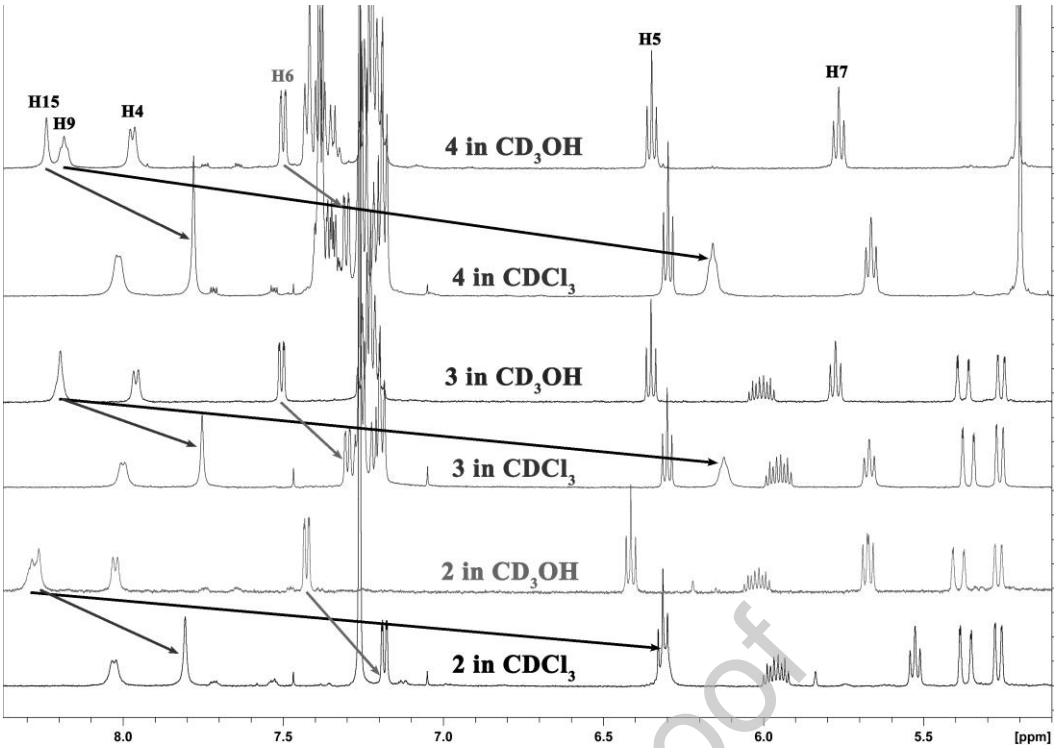

Fig. 2. 1H-NMR profiles of the compounds **2**, **3** and **4** in $CDCl_3$ and CD_3OH. The main differences are highlighted.

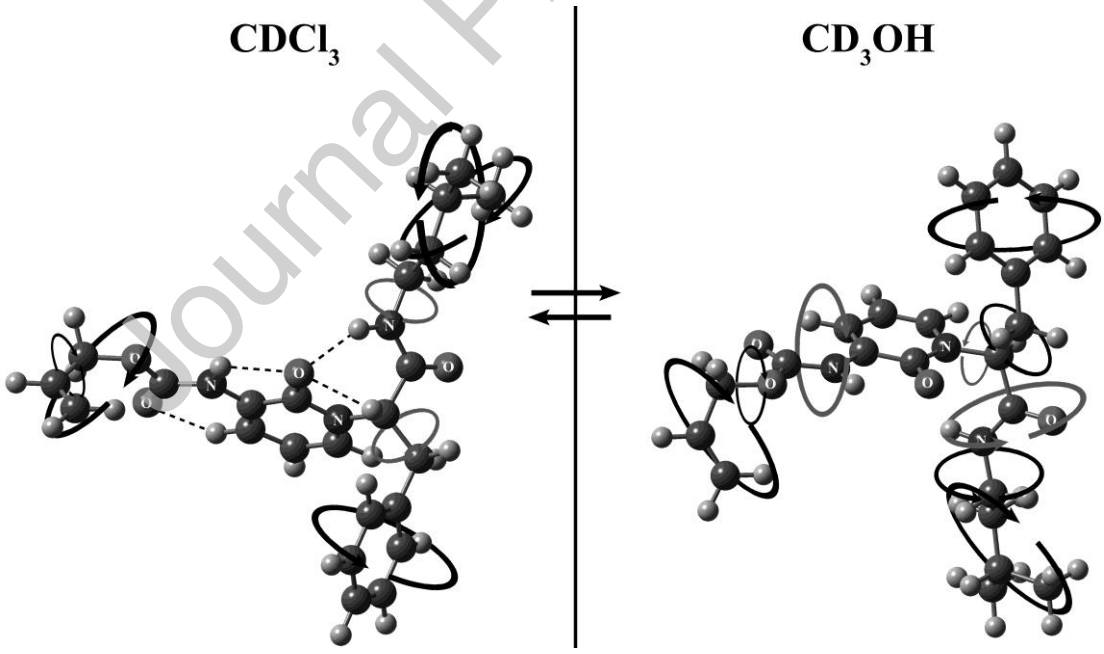

Fig. 3. Schematic conformational representation of **3**, whose conformational freedom results limited in $CDCl_3$ and is enhanced in polar protic solvents like CD_3OH. Darker rotation arrows indicate more dynamic freedom.

3. Material and Methods

3.1. Chemistry

All reagents and solvents were purchased from commercial suppliers and used without any further purification. Elemental analyses were performed on a C. Erba Model 1106 Elemental Analyzer and the results are within ±0.4% of the theoretical values. Merck silica gel 60 F254 plates were used for analytical TLC. Semipreparative HPLC was performed on a Waters 1525 binary HPLC pump system equipped with a Rheodyne model 3725i injector (2 mL sample loop). Reverse-phase chromatography was carried out on a Merck Chromolith SemiPrep RP-18e column (100x10 mm i.d.), at a temperature of 20°C, with a mobile phase of water/acetonitrile (90:10) and a flow rate of 5 mL min^{-1}. A Waters 2489 UV/Vis dual-wavelength absorbance detector was used, and chromatograms were processed using Waters HPLC Breeze 2 software. The detector wavelength was set at 266 and 310 nm. All solutions employed in the analysis were filtered through 25 mm x 0.45 mm polypropylene (PP) membrane. ^{1}H-NMR and ^{13}C-NMR spectra were recorded on a Varian 500 MHz spectrometer operating at 499.74 and 125.73 MHz for ^{1}H-NMR and ^{13}C-NMR spectra, respectively. The residual signal of the deuterated solvent was used as internal standard. Chemical shifts are given in δ (ppm) and coupling constants (*J*) in Hz. Splitting patterns are described as singlet (s), broad singlet (bs), doublet (d), triplet (t), quartet (q), multiplet (m), doublet of doublet (dd), or triplet of doublets (td).

(S)-allyl (1-(1-(isopentylamino)-4-methyl-1-oxopentan-2-yl)-2-oxo-1,2-dihydropyridin-3-yl)carbamate **2**. In a round bottom flask at 0°C and under nitrogen atmosphere, acid **9** (1.0 eq.) was solubilized in DCM/DMF (1:1) and HOBt (1.5 eq) and EDCI (1.5 eq.) were added. After 10 min, DIPEA (2 eq.) and isopentylamine (1.2 eq.) were added and the reaction was stirred at rt overnight. Subsequently, solvents were removed *in* vacuo and the resulting residue was dissolved in EtOAc and washed with 1 M HCl (x3), saturated $NaHCO_3$ solution (x3) and brine (x3), dried over $MgSO_4$, filtered and concentrated under reduced pressure following preliminary purification by flash column chromatography (EtOAc/light petroleum 9/1) and subsequent semipreparative RP-HPLC.

Consistency: white powder; yield: 68%. Rf=0.47 Elemental analysis for $C_{20}H_{31}N_3O_4$: calculated: C 63.64, H 8.28, N 11.13; C 63.79, H 8.52, N 10.84. ^{1}H NMR (500 MHz, chloroform-*d*) δ ppm 0.86 (dd, *J*=6.71, 2.44 Hz, 6 H) 0.90 - 0.96 (m, 6 H) 1.40 - 1.47 (m, 2 H) 1.47 - 1.54 (m, 2 H) 1.83 (ddd, *J*=14.12, 8.32, 5.95 Hz, 1 H) 1.95 - 2.08 (m, 2 H) 3.11 - 3.20 (m, 1 H) 3.21 - 3.35 (m, 2 H) 4.67 (br d, *J*=5.49 Hz, 1 H) 5.27 (br dd, *J*=10.53, 1.07 Hz, 1 H) 5.37 (br dd, *J*=17.24, 1.37 Hz, 1 H) 5.53 (br t, *J*=7.78 Hz, 1 H) 5.91 - 6.01 (m, 1 H) 6.28 - 6.31 (m, 1 H) 6.31 (t, *J*=7.32 Hz, 2 H) 7.18 (dd, *J*=7.02, 1.53 Hz, 1 H) 7.81 (br s, 1 H) 7.96 - 8.09 (m, 1 H). Extensive spectral data are reported in the supportive file.

*(S)-allyl (1-(1-(isopentylamino)-1-oxo-3-phenylpropan-2-yl)-2-oxo-1,2-dihydropyridin-3-yl)carbamate **3**.* Synthesis of **3** was carried out following the same procedure used for **2**, using the intermediate **10** as acid. Consistency: white powder; Yield: 73%. Rf= 0.50 (EtOAc/light petroleum 9/1) Elemental analysis for $C_{23}H_{29}N_3O_4$: calculated: C 67.13, H 7.10, N 10.21; found: C 66.94, H 7.34, N 10.14. ^{1}H NMR (500 MHz, chloroform-*d*) δ ppm 0.82 (dd, *J*=6.60, 1.32 Hz, 6 H) 1.21 - 1.27 (m, 2 H) 1.38 (br dd, *J*=13.43, 6.68 Hz, 1 H) 3.11 (dd, *J*=13.72, 6.82 Hz, 1 H) 3.15 (br s, 1 H) 3.19 - 3.25 (m, 1 H) 3.54 (dd, *J*=13.72, 8.58 Hz, 1 H) 4.66 (d, *J*=5.58 Hz, 1 H) 5.26 (dd, *J*=10.42, 1.03 Hz, 1 H) 5.36 (br dd, *J*=17.24, 1.39 Hz, 1 H) 5.67 (br t, *J*=7.92 Hz, 1 H) 5.86 - 6.02 (m, 2 H) 6.11 (br s, 1 H) 6.30 (t, *J*=7.26 Hz, 1 H) 7.16 - 7.21 (m, 1 H) 7.22 (br d, *J*=7.04 Hz, 1 H) 7.24 - 7.28 (m, 9 H) 7.30 (dd, *J*=7.04, 1.32 Hz, 1 H) 7.75 (s, 1 H) 8.00 (br d, *J*=6.60 Hz, 1 H) Extensive spectral data are reported in the supportive file.

*(S)-benzyl (1-(1-(isopentylamino)-1-oxo-3-phenylpropan-2-yl)-2-oxo-1,2-dihydropyridin-3-yl)carbamate **4**.* Synthesis of **4** was carried out following the same procedure used for **2**, using the intermediate **11** as acid. Consistency: white powder; yield: 77%; R_f = 0.53 (EtOAc/light petroleum 9/1). Elemental analysis for $C_{27}H_{31}N_3O_4$: calculated: C 70.26, H 6.77, N 9.10; C 69.97, H 6.72, N 9.29. ^{1}H NMR (500 MHz, chloroform-*d*) δ ppm 0.81 (dd, *J*=6.72, 1.34 Hz, 6 H) 1.20 - 1.28 (m, 2 H) 1.38 (dq, *J*=13.40, 6.62 Hz, 1 H) 3.08 (s, 1 H) 3.09 - 3.14 (m, 2 H) 3.21 (td, *J*=13.53, 7.23 Hz, 1 H) 3.53 (dd, *J*=13.61, 8.57 Hz, 1 H) 5.20 (s, 1 H) 5.66 (br t, *J*=7.90 Hz, 2 H) 6.16 (br s, 1 H) 6.30 (t,

J=7.23 Hz, 1 H) 7.16 - 7.20 (m, 2 H) 7.22 (br d, *J*=1.34 Hz, 1 H) 7.23 - 7.26 (m, 1 H) 7.30 (dd, *J*=7.06, 1.34 Hz, 1 H) 7.34 - 7.36 (m, 1 H) 7.38 (s, 1 H) 7.38 - 7.41 (m, 2 H) 7.78 (s, 1 H) 7.97 - 8.09 (m, 1 H).

3.2. Conformational analyses

Small amounts of pure compounds **2**, **3** and **4** (0.6, 1.2 and 2.4 mg respectively) were first dissolved in $CDCl_3$ (600 μL) and poured in the 5 mm test tubes in order to run the thorough NMR analysis for the total assignment. After these analyses the same tubes were freeze-dyed under vacuum to eliminate the solvent and re-dissolve the same matter in CD_3OH (650 μL) clearly known as polar and protic solvent mimicking polar media in biological conditions. Again, the complete NMR analyses were accomplished to elicit the elements supporting similar and different features of the conformational behaviour of such species.

^1H, $^{13}C\{^1H\}$ and $^{15}N\{^1H\}$ NMR spectra of **2, 3** and **4** Varian 500 MHz spectrometer equipped with a ONE_NMR probe and operating at 499.74, 125.73, 50.65 MHz respectively. For $CDCl_3$ solutions calibration was set according to signals of the added standard TMS (tetra-methyl-silane; δH= 0.00 ppm; δC= 0.00 ppm); for CD_3OH calibration is fixed using the residual proton signals of $CD_2\mathit{H}OH$ (δH= 3.30 ppm) and the solvent septuplet ^{13}C resonance (δC= 39.52ppm). ^{15}N calibration was referred to the CH_3NO_2 as external standard (90% CH_3NO_2 in CD_3OH δ = 380.5 ppm). Complete and unambiguous assignment was pursued by several 1D and 2D homo- and hetero-nuclear NMR experiments such as 2D-TOCSY, 2D-NOESY or ROESY, ^{13}C-HSQC, ^{13}C-HMBC, ^{15}N-HSQC and ^{15}N-HMBC (Tables **2-4**). In order to summarize all the data related to molecular structures we have used the ACD/lab 2012 free version. Extended material is reported into the supplementary data. In order to support the detected conformation of compound **3** we have used GAUSSIAN03 software package for modeling and DFT B3LYP method with G6-31 basis sets for energy optimization. Two stable conformations changing dihedral angle around the N1-C7 bond were explored. As expected, the conformation close to the main conformation detected in $CDCl_3$ in

Fig. (**3**) was about 18.43 kJ/mol, in the gas phase, more stable than the best found alternative (the two minimized structures reported in Section 4 show an energy gap of 0.00702 Hartrees equal to 18.43 kJ/mol). It is supporting the overall discussion concerning the conformational analysis.

3.3. In vitro 20S immunoproteasome/proteasome inhibition assays

Human 20S immunoproteasome, obtained from human spleen, and human 20S proteasome, isolated from human erythrocytes, were purchased from Enzo Life Science. The hydrolysis of the appropriate peptidyl 7-amino-4-methyl-coumarin substrate was monitored to measure the different proteolytic activities of both proteasome and immunoproteasome. The substrates Suc-Leu-Leu-Val-Tyr-AMC (Bachem) for β5c-β5i, Boc-Leu-Arg-Arg-AMC (Bachem) for β2c-β2i, Z-Leu-Leu-Glu-AMC (Adipogen) for β1c and Ac-Pro-Ala-Leu-AMC (Biomol GmbH) for β1i subunits were employed at 50 μM, with the exception of Z-Leu-Leu-Glu-AMC (80 μM). Fluorescence of the product AMC of the substrate hydrolyses was measured at 30°C with a 380 nm excitation filter and a 460 nm emission filter, using an Infinite 200 PRO microplate reader (Tecan, Männedorf, Switzerland). A preliminary screening at 50 μM inhibitor concentrations was carried out on the three proteolytic activities of proteasome and immunoproteasome; an equivalent amount of DMSO as a negative control and MG-132 (a reversible inhibitor of immunoproteasome) as positive control were employed. Compounds showing at least 60% inhibition at the screening concentration were then progressed into detailed assays. Continuous assays were performed at seven different concentrations ranging from those that minimally inhibited to those that fully inhibited each proteolytic activity to calculate the dissociation constants K_i of the enzyme-inhibitor complex by means of the Cheng-Prusoff equation $K_i = IC_{50}/(1 + [S]\ K_m^{-1})$. Inhibitor solutions were prepared from stocks in DMSO. Each independent assay was performed in duplicate in 96-well-plates in a total volume of 200 μL. For the assay on β5i, β1i, β1c and β5c subunits, human 20S immunoproteasome or human 20S proteasome was incubated at 30°C obtaining a final concentration of 0.004 mg/mL with the inhibitor at seven different concentrations. The reaction buffer comprised: 50 mM Tris HCl, pH 7.4, 25 mM KCl, 10 mM NaCl, 1 mM $MgCl_2$, 0.03% SDS.

AMC released from substrate hydrolysis was monitored in kinetic cycle over a period of 10 min. For the assay on β2i and β2c subunits, final concentration of immunoproteasome or proteasome was of 0.0025 mg/mL. The reaction buffer comprised: 50 mM Tris HCl, pH 7.4, 0.5 mM EDTA III, 50 mM NaCl, 0.03% SDS.

4. Conclusions

This study is based on novel derivatives generated from a lead compound with the purpose to design an active inhibitor against immunoproteasome with specific selectivity toward the important β5i subunit, i.e compound **3**. In this context three compounds with different substitution pattern were synthesized and tested *in vitro* for their biological activity. In order to find out the rationale of the obtained results we achieved an extensive hetero-nuclear NMR analysis taking advantage of a careful global evaluation of many data processed in paragraph 2 (see also supporting information). As expected, given a thermodynamically favoured conformation, all of the three molecules present a certain dynamic freedom in CD_3OH which is a protic solvent mimicking biological polar media. On the other hand, in the apolar solvent $CDCl_3$ the conformational freedom is greatly reduced by the clear detection of dipolar intramolecular interactions; interestingly this trend is definitely more pronounced for the more active and selective compound. The conformational stiffness in apolar media accounts for the thermodynamic advantage of this construct to enter the macromolecular apolar binding site, still keeping the necessary kinetic mobility coming from the polar (water-like) biological media. This strategy can be adopted to study also many other biologically active molecules.

List of Abbreviations

CPs = constitutive core particles

C-L = caspase-like

T-L = trypsin-like

ChT-L = chymotrypsin-like

iCPs = immuno-core particles

MM = multiple myeloma

Phe = phenylalanine

Leu = leucine

DCM= dichoromethane

DMF = dimethylformamide

HOBt= *Hydroxybenzotriazole*

EDCI=*N*-Ethyl-*N*2-(3-dimethylaminopropyl)carbodiimide hydrochloride

DIPEA= *N*,*N*-diisopropylethylamine

NMR = Nuclear Magnetic Resonance

NOESY = nuclear Overhauser effect spectroscopy

2D = two-dimensional

ROESY = rotating-frame Overhauser effect spectroscopy

HSQC = hetero-nuclear single quantum coherence spectroscopy

HMBC = hetero-nuclear multi-bond correlation spectroscopy

TMS = Tetra-Methyl-Sylane

EDTA = Ethylene-diamino-tetra-acetic acid

SDS = sodium dodecyl sulphate

Acknowledgements

This work was financially supported by the Ministero dell'Istruzione, dell'Universita' e della Ricerca Scientifica e Tecnologica [MIUR-PRIN2010-2011, grant 2010W7YRLZ_004 (M.Z.)].

Declaration of interests

x The authors declare that they have no known competing financial interests or personal relationships that could have appeared to influence the work reported in this paper.

☐The authors declare the following financial interests/personal relationships which may be considered as potential competing interests:

CREDIT AUTHOR STATEMENT

Archimede Rotondo: Conceptualization, Methodology, Software, Writing,Original draft preparation, final editing. **Maria Zappalà**: Supervision, coordination. **Santo Previti**: Data extraction, writing collaboration. ***Carla Di Chio****:* Data analysis (pharmacological)**. Alessandro Allegra**: Data analysis (pharmacological): **Roberta Ettari:** Co-Writing, Co-Editing, Co Supervising

Supplementary Material Content

Section 1. Detailed NMR analysis.

Section 2. Extended spectra and data concerning compound **2** in $CDCl_3$ and in CD_3OD

Section 3. Extended spectra and data concerning compound **3** in $CDCl_3$ and in CD_3OD

Section 4. Extended spectra and data concerning compound **4** in $CDCl_3$ and in CD_3OD

Section 5. Gaussian optimization (DFT B3LYP methods with 6/3/1 G basis sets) for compound **3** in two different conformations

References

[1] S.H. Lecker, A.L. Goldberg, W.E: Mitch, Protein degradation by the ubiquitin–proteasome pathway in normal and disease states, JASN 17 (2006**)** 1807-1819. https://doi.org/10.1681/ASN.2006010083.

[2] G.N De Martino, T.G. Gillette, Proteasomes: machines for all reasons, Cell 129 (2007) 659–662. https://doi.org/10.1016/j.cell.2007.05.007.

[3] N. Micale, K. Scarbaci, V. Troiano, R. Ettari, S. Grasso, M. Zappalà, Peptide-based proteasome inhibitors in anticancer drug design, Med. Res. Rev. 34 (2014) 1001-1069. https://doi.org/10.1002/med.21312.

[4] A. Ciechanover, A.L. Schwartz, The ubiquitin system: pathogenesis of human diseases and drug targeting, Biochim. Biophys. Acta 1695 (2004) 3-17. https://doi.org/10.1016/j.bbamcr.2004.09.018.

[5] A.F. Kisselev, W.A. van der Linden, H.S. Overkleeft, Proteasome inhibitors: an expanding army attacking a unique target, Chem. Biol. 19 (2012) 99–115. https://doi.org/10.1016/j.chembiol.2012.01.003.

[6] C. Montagut, A. Rovira, J. Albanell, The proteasome: a novel target for anticancer therapy, Clin. Transl. OncoL 8(5) (2006) 313-7 313

[7] H. Huang, D. Chen, S. Li, X. Li, N. Liu, X. Lu, S Liu, K. Zhao, C. Zhao, H. Guo, C. Yang, P. Zhou, X. Dong, C. Zhang, G. Q. Ping Dou, J. Liu, Gambogic acid enhances proteasome inhibitor-induced anticancer activity, Cancer Letters 301 (2011) 221–228.

[8] M. Groll, L. Ditzel, J. Lowe, D. Stock, M. Bochtler, H.D. Bartunik, R. Huber, Structure of 20S proteasome from yeast at 2.4 A resolution, Nature 386 (1997) 463–471. https://doi.org/10.1038/386463a0.

[9] E.M. Huber, M. Basler, R. Schwab, W. Heinemeyer, C.J. Kirk, M. Groettrup, M. Groll, Immuno- and constitutive proteasome crystal structures reveal differences in substrate and inhibitor specificity, Cell 148 (2012) 727–738. https://doi.org/10.1016/j.cell.2011.12.030.

[10] R. Ettari, S. Previti, A. Bitto, S. Grasso, M. Zappalà, Immunoproteasome-selective inhibitors: a promising strategy to treat hematologic malignancies, autoimmune and inflammatory diseases, Curr. Med. Chem. 23 (2016) 1217-1238. https://doi.org/10.2174/0929867323666160318173706.

[11] D.J. Kuhn, S.A. Hunsucker, Q. Chen, P.M. Voorhees, M. Orlowski, R.Z. Orlowski, Targeted Targeted inhibition of the immunoproteasome is a potent strategy against models of multiple myeloma that overcomes resistance to conventional drugs and nonspecific proteasome inhibitors, Blood 113 (2009) 4667–4676. https://doi.org/10.1182/blood-2008-07-171637.

[12] E.M. Huber, M. Groll, Inhibitors for the immuno- and constitutive proteasome: current and future trends in drug development, Angew. Chem. Int. Ed. Engl. 51 (2012) 8708–8720. https://doi.org/10.1002/anie.201201616.

[13] R. Ettari, M. Zappalà, S. Grasso, C. Musolino, V. Innao, A. Allegra, Immunoproteasome-selective and non-selective inhibitors: a promising approach for the treatment of multiple myeloma, Pharmacol. Ther. 182 (2018) 176-192. https://doi.org/10.1016/j.pharmthera.2017.09.001.

[14] M. Kaiser, M. Groll, C. Siciliano, I. Assfalg-Machleidt, E. Weyher, J. Kohno, A.G. Milbradt, C. Renner, R. Huber, L. Moroder, Binding mode of TMC-95A analogues to eukaryotic 20S proteasome, ChemBioChem 5 (2004), 1256-1266. https://doi.org/10.1002/cbic.200400096.

[15] M. Groll, N. Gallastegui, X. Maréchal, V. Le Ravalec, N. Basse, N. Richy, E. Genin, R. Huber, L. Moroder, J. Vidal, M. Reboud-Ravaux, 20S proteasome inhibition: designing noncovalent linear peptide mimics of the natural product TMC-95A, ChemMedChem 5 (2010) 1701-1705. https://doi.org/10.1002/cmdc.201000293.

[16] N. Gallastegui, P. Beck, M. Arciniega, R. Huber, S. Hillebrand, M. Groll, Hydroxyureas as noncovalent proteasome inhibitors, Angew Chem Int Ed Engl. 51 (2012) 247-249. https://doi.org/10.1002/anie.201106010.

[17] R.L.A. Santos, L. Bai, P.K. Singh, N. Murakami, H. Fan, W. Zhan, Y. Zhu, X. Jiang, K. Zhang, J.P. Assker, C.F. Nathan, H. Li, J. Azzi, G. Lin, Structure of human immunoproteasome with a reversible and noncompetitive inhibitor that selectively inhibits activated lymphocytes. Nat. Commun. 8 (2017), 1692. https://doi.org/10.1038/s41467-017-01760-5.

[18] R. Ettari, C. Bonaccorso, N. Micale, C. Heindl, T. Schirmeister, M.L. Calabrò, S. Grasso, M. Zappalà, Development of novel peptidomimetics containing a vinyl sulfone moiety as proteasome inhibitors, ChemMedChem 6 (2011) 1228–1237. https://doi.org/10.1002/cmdc.201100093.

[19] N. Micale, R. Ettari, A. Lavecchia, C. Di Giovanni, K. Scarbaci, V. Troiano, S. Grasso, E. Novellino, T. Schirmeister, M. Zappalà, Development of peptidomimetic boronates as proteasome inhibitors, Eur. J. Med. Chem. 64 (2013) 23–34. https://doi.org/10.1016/j.ejmech.2013.03.032.

[20] K. Scarbaci, V. Troiano, N. Micale, R. Ettari, L. Tamborini, C. Di Giovanni, C. Cerchia, S. Grasso, E. Novellino, T. Schirmeister, A. Lavecchia, M. Zappalà, Identification of a new series of amides as non-covalent proteasome inhibitors, Eur. J. Med. Chem. 76 (2014) 761–769. https://doi.org/10.1016/j.ejmech.2014.01.022.

[21] V. Troiano, K. Scarbaci, R. Ettari, N. Micale, C. Cerchia, A. Pinto, T. Schirmeister, E. Novellino, S. Grasso, A. Lavecchia, M. Zappalà, Optimization of peptidomimetic boronates bearing a P3 bicyclic scaffold as proteasome inhibitors, Eur. J. Med. Chem. 83 (2014) 1–14. https://doi.org/10.1016/j.ejmech.2014.06.017.

[22] K. Scarbaci, V. Troiano, R. Ettari, A. Pinto, N. Micale, C. Di Giovanni, C. Cerchia, T. Schirmeister, E. Novellino, A. Lavecchia, M. Zappalà, S. Grasso, Development of novel selective peptidomimetics, containing a boronic acid moiety, targeting the 20S proteasome as anticancer agents, ChemMedChem 9 (2014) 1801–1816. https://doi.org/10.1002/cmdc.201402075.

[23] C. Di Giovanni, R. Ettari, S. Sarno, A. Rotondo, A. Bitto, F. Squadrito, D. Altavilla, T. Schirmeister, E. Novellino, S. Grasso, M. Zappalà, A. Lavecchia, Identification of noncovalent proteasome inhibitors with high selectivity for chymotrypsin-like activity by a multistep structure-based virtual screening, Eur. J. Med. Chem. 121 (2016), 578–591. https://doi.org/10.1016/j.ejmech.2016.05.049.

[24] R. Ettari, G. Pallio, G. Pizzino, N. Irrera, M. Zappalà, S. Maiorana, C. Di Chio, D. Altavilla, F. Squadrito, A. Bitto, Noncovalent immunoproteasome inhibitors induce cell cycle arrest in multiple myeloma cells, J. Enzyme Inhib. Med. Chem. 34 (2019) 1307–1313. https://doi.org/10.1080/14756366.2019.1594802.

[25] R. Ettari, C. Cerchia, S. Maiorana, M. Guccione, E. Novellino, A. Bitto, S. Grasso, A. Lavecchia, M. Zappalà, Development of novel amides as noncovalent inhibitors of immunoproteasomes, ChemMedChem 14 (2019) 842 – 852. https://doi.org/10.1002/cmdc.201900028.

[26] A. Rotondo, R. Ettari, M. Zappalà, C. De Micheli, E. Rotondo, NMR Characterization and conformational analysis of a potent papain-family cathepsin L-like cysteine protease inhibitor with different behaviour in polar and apolar media, J. Mol. Struct. 1076 (2014), 337–343. https://doi.org/10.1016/j.molstruc.2014.07.046.

[27] A. Rotondo, R. Ettari, S. Grasso, M. Zappalà, NMR conformational analysis in solution of a potent class of cysteine proteases inhibitors, Struct. Chem. 26 (2015) 943–949. https://doi.org/10.1007/s11224-015-0597-5.

[28] K. Gaalswyk, C.N. Rowley, An explicit-solvent conformation search method using open software, PeerJ 4 (2016) e2088. https://doi.org/10.7717/peerj.2088.

[29] R.A. Copeland, Conformational adaptation in drug–target interactions and residence time, *Fut. Med. Chem.* 3 **(2011)** 1491-1501. https://doi.org/10.4155/fmc.11.112.

[30] E.M. Larsena, M.R. Wilson, R.E. Taylor, Conformation-activity relationships of polyketide natural products, Nat. Prod. Rep. 32 (2015) 1183–1206. https://doi.org/10.1039/C5NP00014A.

[31] A. Balaban, Drug design, molecular descriptors in encyclopedia of complexity and systems science, Springer Science+Business Media New York (2014). https://doi.org/10.1007/978-3-642-27737-5_136-2.

GRAPHICAL ABSTRACT